Numerical and Experimental Characterisation of Interactions Between two Marine Current Turbines

Paul MYCEK [1,2], Benoît GAURIER [2], Grégory GERMAIN [2], Corentin LOTHODÉ [1,2], Grégory PINON [1], Élie RIVOALEN [1,3]

1. Université du Havre, UFR Sciences et Techniques, UMR 6294 CNRS - LOMC, 53 rue de Prony, BP 540, 76058 Le Havre, France. *gregory.pinon@univ-lehavre.fr*
2. IFREMER, Centre Manche Mer du Nord, Service Hydrodynamique et Océanométéo, 150 quai Gambetta, BP 699, 62321 Boulogne-sur-Mer, France. *{paul.mycek, benoit.gaurier, gregory.germain}@ifremer.fr*
3. INSA de Rouen, EA 3828 - LOFIMS, Avenue de l'Université, BP 08, 76801 Saint-Étienne-du-Rouvray, France. *elie.rivoalen@insa-rouen.fr*

Abstract:
The implantation and deployment of marine current turbine arrays depend on the understanding of their interactions. Based on *a priori* suggestions about the layout of marine energy converter arrays, we propose to highlight interactions effects between two horizontal axis marine current turbines, in open water.
Experimental trials were run in IFREMER's wave and current flume tank in Boulogne-sur-Mer (France), on marine current turbine models. Our study focuses on setups were the second turbine is axially aligned, at different distances, in the wake of the first one. Interaction effects are pointed out both in terms of performance and wake characterisation by means of a comparison with results on a single turbine. This study shows that the downstream turbine behaviour is deeply influenced by the upstream turbine wake.
We also present numerical results obtained on a single turbine from our tri-dimensional numerical software, which is developed at the *Laboratoire Ondes et Milieux Complexes*, Le Havre (France). Those numerical results are validated by the comparison with the experiments, which allows us to foresee the modelling of several turbines and thus of turbine farms with a more complex layout.

Keywords:
Marine energy – Horizontal axis Marine Current Turbines – Turbine arrays – Experimental trials – Laser Doppler Velocimetry – Numerical simulation – Vortex method

1. Introduction

Marine current turbines behaviour, subject to different flow conditions, has now become well documented, mostly thanks to experimental (BATTEN *et al.*, 2008 ; MAGANGA *et al.*, 2010) or numerical studies (BALTAZAR & FALCÃO DE CAMPOS, 2008 ; PINON *et al.*, 2012). However, while numerous projects concerning the implantation of turbine arrays are being launched, the interaction issue remains little discussed in the scientific literature.

It is likely that the implantation of marine current turbine arrays will be carried out in two steps. First, such arrays will only consist of one row, or two shifted rows so that no negative interaction occurs. Such farms are called first generation arrays. However, new rows will have to be implanted in order to increase the number of turbines. Negative interactions, due to the upstream turbines wakes and perceived by the downstream turbines, will then be unavoidable (see figure 1). These are called second generation arrays (MYERS *et al.*, 2010 ; RAWLINSON-SMITH *et al.*, 2010).

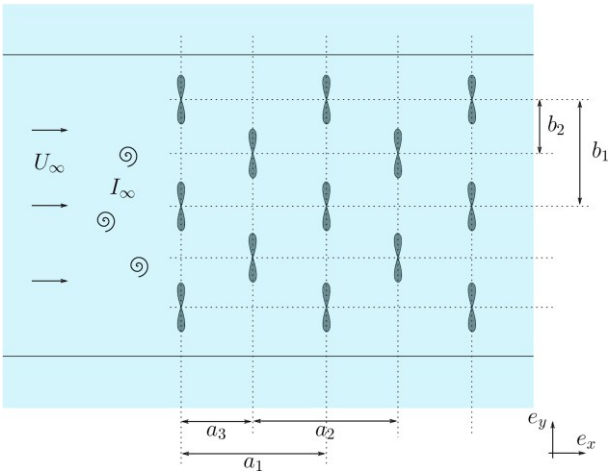

Figure 1. Schematic top view of a turbine array with the different layout parameters involved.

Although one may find some *a priori* suggestions regarding the implantation of marine energy converter arrays (MYERS *et al.*, 2010 ; RAWLINSON-SMITH *et al.*, 2010), to the athors' knowledge, no real operating conditions study has been carried out to this day on horizontal axis turbines. We propose to mark a first milestone by studying the interactions between two marine current turbines, located one behind the other.

In the first part of this work, we present numerical and experimental results on a single turbine, which are used in the second part in order to point out the existence of interaction effects between two aligned turbines.

2. Single turbine setup

The behaviour of a marine current turbine is subject to several parameters, amongst others:

- The upstream velocity, uniform in this study, denoted by U_∞;
- The Tip Speed Ratio (TSR), defined as the ratio between the tip velocity and the upstream velocity U_∞:

$$\mathrm{TSR} = \frac{\Omega R}{U_\infty}, \tag{1}$$

where $R = D/2$ is the rotor radius and Ω its rotation speed;

- The ambient turbulence intensity rate (TI_∞), defined by:

$$\mathrm{TI}_\infty = 100 \times \frac{\sqrt{u'^2 + v'^2 + w'^2}}{\sqrt{\overline{u}^2 + \overline{v}^2 + \overline{w}^2}}, \tag{2}$$

where u, v, w are the three vector velocity components, $\overline{q}$ denotes the time-averaged value and q' the standard deviation of any quantity q.

Trials were run in IFREMER's flume tank in Boulogne-sur-Mer (France), on a 1/30 scale model of a turbine prototype. Figure 2 depicts a schematic view of the experimental setup. Wake measurements were performed with a LDV (Laser Doppler Velocimetry) system, while the force and moment were measured with a six-components load cell (three force and three moments components).

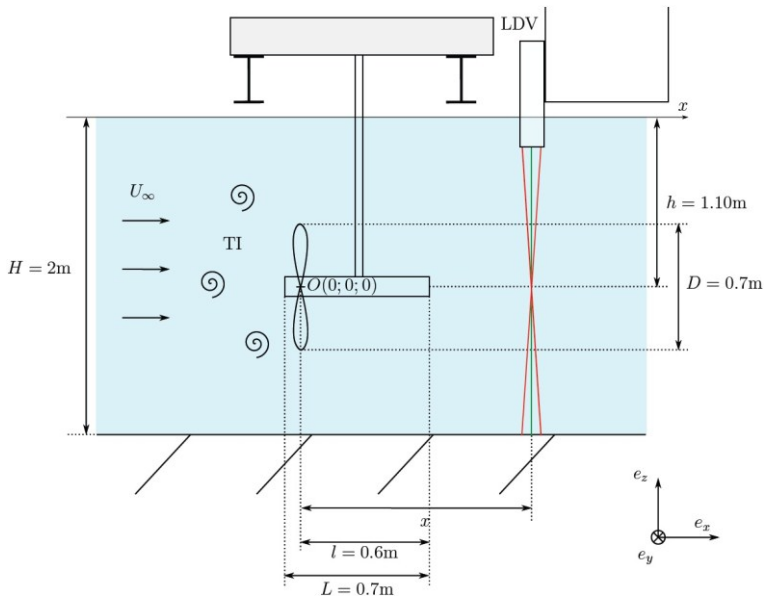

Figure 2. Schematic view of the experimental setup.

The flume tank is $18 \times 4 \times 2\,\mathrm{m}$, which is large enough to neglect any blockage effect. The turbine model description is given in table 1.

Table 1. Turbine model description.

Feature	***Description***
Blade profile	*NACA63418*
Rotor diameter (D)	*700mm*
Hub diameter	*92mm*
Hub length	*700mm*
Studied TSR	*[0;10]*
Directrion of rotation	*Counter-clockwise*
Reynolds ($\mathrm{Re}_\infty = U_\infty R/\nu$)	*$\approx$280 000*

2.1 Wake characterisation

By means of the LDV system, the mean velocity is evaluated at different locations downstream of the turbine. With a fine enough grid, wake maps may thus be drawn. Figure 3 shows two downstream axial velocity maps; the first one (figure 3(a)) corresponds to a flow with a 5% turbulence intensity rate TI_∞, while the second one (figure 3(b)), corresponds to a flow with a much higher TI_∞ (25%). These maps point out that the ambient turbulence conditions deeply influence the turbine behaviour. As a matter of fact, with the highest TI_∞ (25%), the downstream flow tends to recover its uniformity and its initial upstream velocity from seven diameters behind the tubine; on the contrary, with a 5% TI_∞, the wake remains well pronounced even ten diameters behind the turbine.

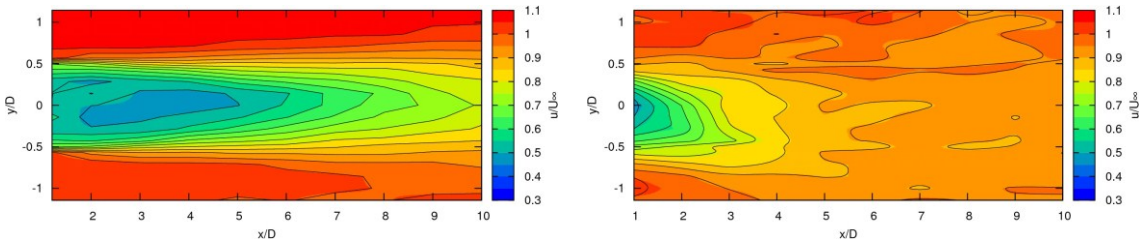

(a) TI_∞ = 5% *(b) TI_∞ = 25%*

Figure 3. Axial velocity maps for two different TI_∞, with TSR = 3.67.

The downstream turbulence can be evaluated in the $(O;x;y)$ plane by the downstream turbulence intensity rate, denoted by TI, and defined by:

$$\mathrm{TI} = 100 \times \frac{\sqrt{u'^2 + v'^2}}{\sqrt{\bar{u}^2 + \bar{v}^2}}. \qquad (3)$$

Thus, TI maps may be drawn downstream of the turbine in a flow with a 5% TI_∞ (figure 4(a)) or a 25% TI_∞ (figure 4(b)). These maps confirm the deep influence of the ambient turbulence and show, once again, that in a flow with a weak turbulence

intensity, the disturbance caused by the turbine remains pronounced over more than ten diameters downstream (MAGANGA, 2011).

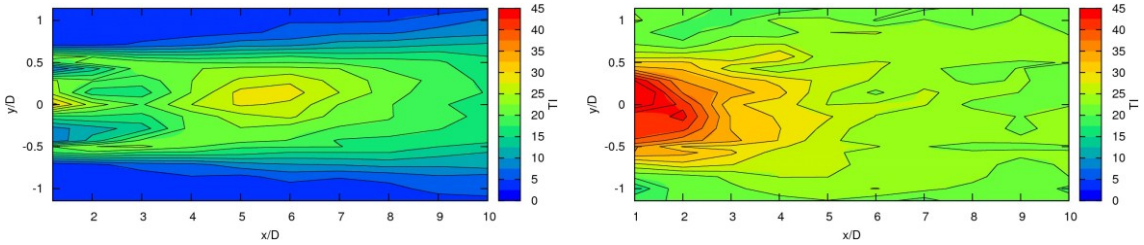

(a) $TI_\infty = 5\%$ *(b)* $TI_\infty = 25\%$

Figure 4. Turbulence intensity maps for two different TI_∞*, with TSR = 3.67.*

From these profiles, the axial velocity mean value $\hat{u}$ can be assessed at some distance x from the turbine, by integrating the axial velocity on the turbine influence area, of radius R^*, at this distance:

$$\hat{u}(x) = \frac{1}{\left(R^*\right)^2} \int_{-R^*}^{+R^*} |y| u(x, y) dy. \quad (4)$$

In fact, this corresponds to an axi-symmetric approximation of the velocity integrated on the R^* radius disc, defined in the plane perpendicular to the turbine axis. Its centre is located on the turbine axis, at a distance x from the latter. Here, R^* is chosen a bit larger than R so as to take the whole velocity deficit into account. The mean deficit at x is then basically given by:

$$\gamma(x) = 100 \times (1 - \hat{u}(x) / U_\infty). \quad (5)$$

This quantity allows us to better compare our numerical and experimental results. The software is developed in the *Laboratoire Ondes et Milieux Complexes* of University of Le Havre, by our team. It is based on a vortex method and is described in detail in (PINON *et al.*, 2005 ; PINON *et al.*, 2012).

Figure 5 depicts a numerical axial velocity map, for a 0% equivalent TI_∞ (figure 5(a)), and the velocity deficit comparison with the experiments (figure 5(b)). The numerical results agree globally well with the the experimental results. The observed discrepancies come from the fact that ambient turbulence cannot be modelled yet in the software, and that its turbulence model for the downstream wake is not sophisticated enough.

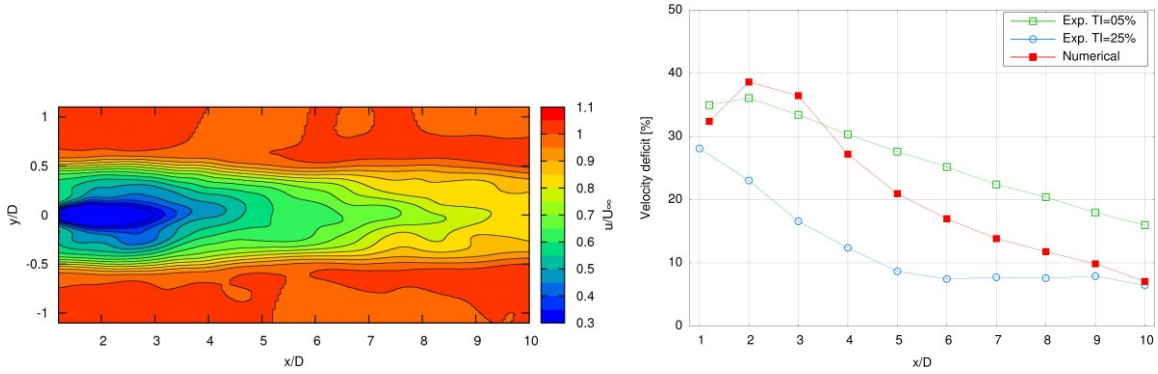

(a) Numerical axial velocity map (TI_∞ =0%)

(b) Axial velocity deficit evolution function of the distance from the turbine

Figure 5. Numerical wake characterisation, with TSR=3.67.

2.2 Turbine performance

The turbine performance can be assessed by its power coefficient, defined by:

$$C_P = \frac{M_x \Omega}{\frac{1}{2}\rho \pi R^2 U_\infty^3} \tag{6}$$

where M_x denotes the rotor axial moment.

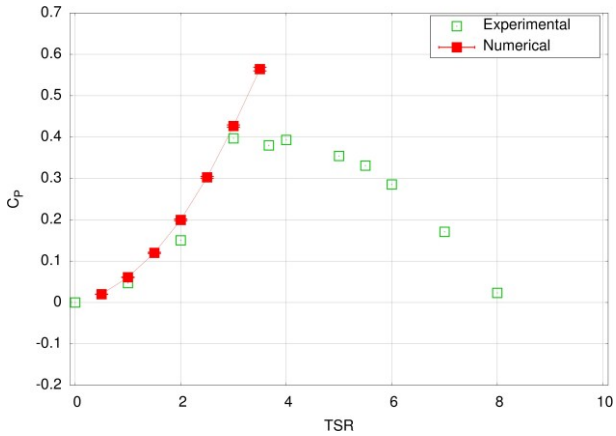

Figure 6. C_P evolution function of the TSR (TI_∞ = 5% for the experiment).

Figure 6 shows the turbine power coefficient evolution function of its TSR. The operating point is reached between TSR = 3 and TSR = 4, with about 40% recovered energy ($C_P = 0{,}4$). The numerical evolution matches the experimental evolution until TSR = 3. The fact that the numerical C_P keeps increasing stems from our particle emission scheme, which does not model flow separation on the blades.

Likewise, the thrust coefficient might be considered function of the TSR. This coefficient, denoted by C_T, is defined by:

$$C_T = \frac{F_x}{\frac{1}{2}\rho \pi R^2 U_\infty^2} \tag{7}$$

where F_x denotes the axial force on the blades.

Figure 7 presents the turbine thrust coefficient function of its TSR. Once again, and for similar reasons, the numerical evolution ceases to match the experimental evolution from TSR = 3.5.

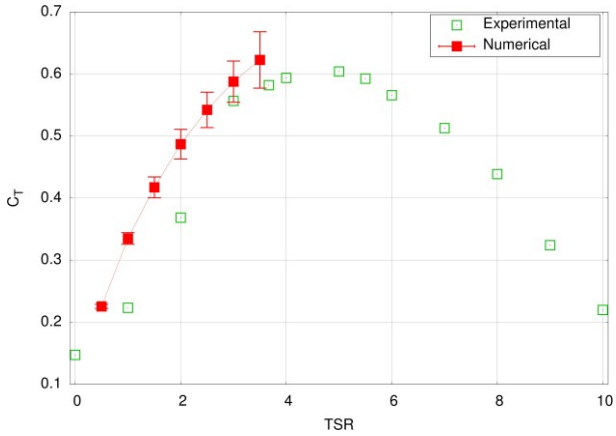

Figure 7. C_T evolution function of the TSR (TI_∞ = 5% for the experiment).

3. Interactions between two turbines

Our study focuses on the interactions between two turbines located one in the wake of the other. The rotor axes are aligned with the flow, as shows figure 8, which describes the experimental setup. The distance between the turbines is denoted by a. Figure 9 shows a picture of this setup.

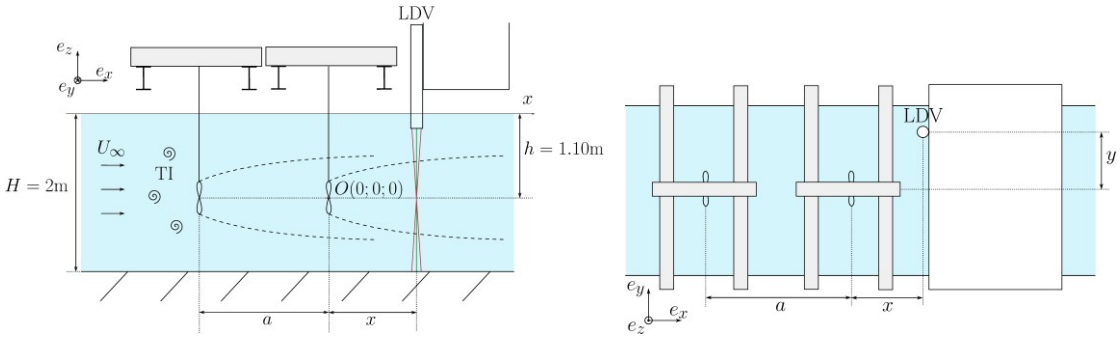

(a) Side view *(b) Top view*

Figure 8. Schematic views of the experimental setup.

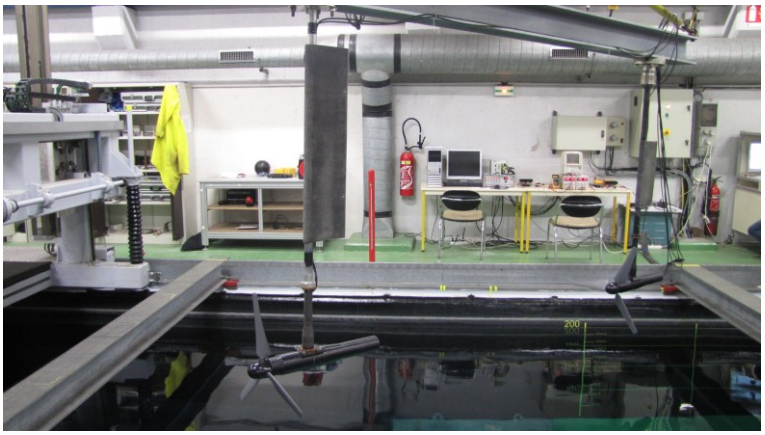

Figure 9. Picture of the experimental setup.

Figure 10(a) shows the axial velocity map behind the downstream turbine, located $4D$ behind the first one. The upstream TI_∞, measured ahead of both turbines, equals 5%. On the other hand, the TI measured $4D$ downstream of a single turbine, in a flow with a 5% TI_∞, equals 25%. Consequently, one might expect to observe, behind the second turbine, a wake similar to the one of a single turbine in a flow with a 25% TI_∞ (figure 3(b)). The significant difference between those two maps (10(a) and 3(b)) points out the interaction effect between the turbines. This conclusion is confirmed by the differences between maps 10(b) and 3(b).

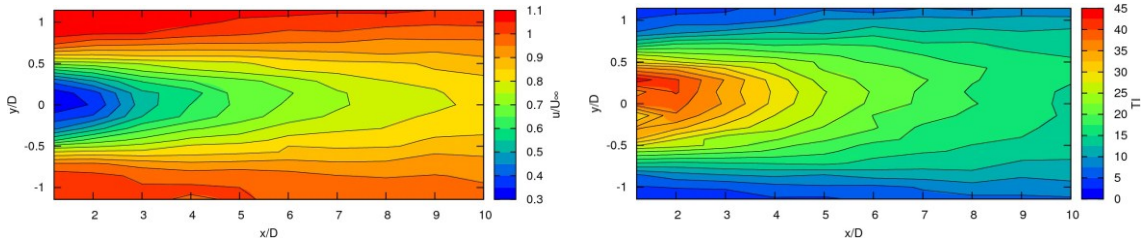

(a) Axial velocity map *(b) Turbulence intensity map*

Figure 10. Axial velocity and turbulence intensity maps downstream of the turbine, with $TI_\infty = 5\%$. The turbines are spaced with $a = 4D$.

Regarding performances, figure 11 shows the turbine C_P^{down} function of its TSR_{down}, for different a/D values. The TSR_{down} is computed from expression (1), that is to say still with regard to the upstream flow velocity U_∞. Likewise, the C_P^{down} is computed from equation (6), with regard to U_∞. In a way, TSR_{down} and C_P^{down} may be considered as incorrect notations. The actual velocity assessment at the downstream turbine location would allow the computation of more physically meaningful downstream TSR and C_P. Nevertheless, our choice is justified by the fact that they represent *indicators*, only based on the known upstream flow conditions, thus allowing the *a priori* apprehension of a turbine farm implantation, where only the ambient site conditions would be known.

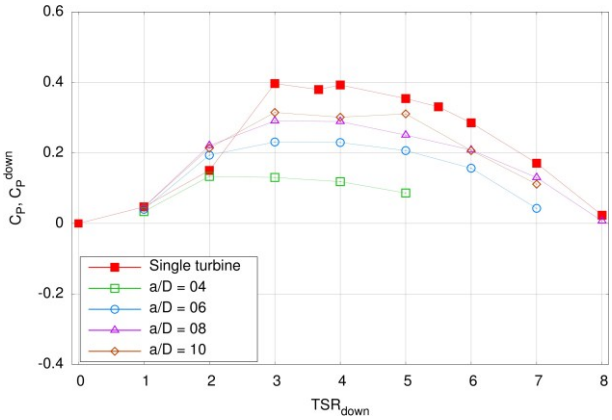

Figure 11. Downstream turbine C_P^{down} evolution function of its TSR_{down}, with the upstream turbine $\mathrm{TSR}_{\mathrm{up}} = 3$ and $TI_\infty = 5\%$.

The comparison with the single turbine C_P (figure 11) points out that the influence of the upstream turbine on the downstream turbine decreases as the distance a/D increases. Ten diameters downstream of the first turbine ($a/D = 10$), the downstream turbine recovers almost the same behaviour as a single turbine for the considered TI_∞.

Let the efficiency η be defined as the ratio between the maximal downstream turbine power coefficient and the power coefficient of a single turbine with TSR = 3:

$$\eta = \frac{\max\left(C_P^{down}\left(\mathrm{TSR}_{\mathrm{down}}\right)\right)}{\max\left(C_P^{up}\left(\mathrm{TSR}_{\mathrm{up}}\right)\right)} = \frac{\max\left(C_P^{down}\left(\mathrm{TSR}_{\mathrm{down}}\right)\right)}{C_P^{\mathrm{single}}\left(\mathrm{TSR}=3\right)}. \quad (8)$$

Figure 12 shows the efficiency η evolution function of the inter-device spacing. This efficiency increases with the distance to reach only 80% for a ten diameters distance between the turbines.

These results point out that, in a second generation array, a compromise should be made between the upstream turbines individual performance of and the inter-device distance. This distance is directly linked to the number of turbines in a given area.

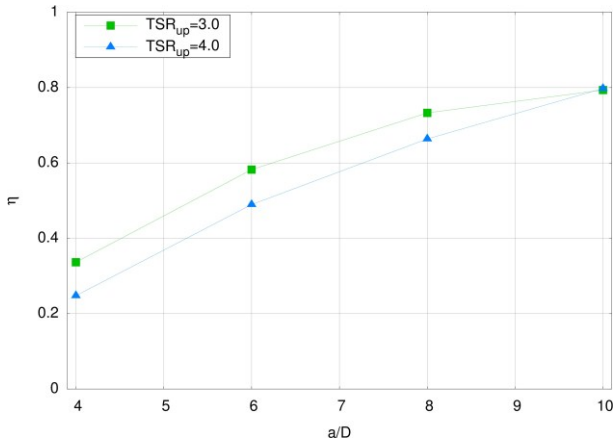

Figure 12. Efficiency η (equation (8)) of the downstream turbine, function of the distance a for upstream TSR of 3 or 4 and $TI_\infty = 5\%$.

4. Conclusions and prospects

This studied has pointed out the existence of interaction effects between two marine current turbines, aligned in a uniform flow. More particularly, with a 5% TI_∞, the wake remains pronounced far behind the turbine in terms of axial velocity deficit, which directly impacts the downstream turbine efficiency (only 80% for a ten diameters inter-device spacing). The performance results thus show that a compromise is necessary between individual device performance and inter-device spacing.

Future work will mainly consist in expanding and improving the numerical software to include a more sophisticated turbulence model and so as to model more than one turbine. Figure 13 illustrates an eight turbines farm, modelled with our numerical tool. However, the discretisation is yet not fine enough to provide physical and converged results.

New experimental trials are planned as well, especially on wake characterisation studies behind two turbines in a 25% TI_∞ upstream flow. In fact, a higher turbulence intensity rate should help the destruction of the coherent vortical structures generated by the turbines. Thus, the downstream turbine behaviour would be less influenced by the upstream turbine wake and the two turbines could then be implanted closer to each other.

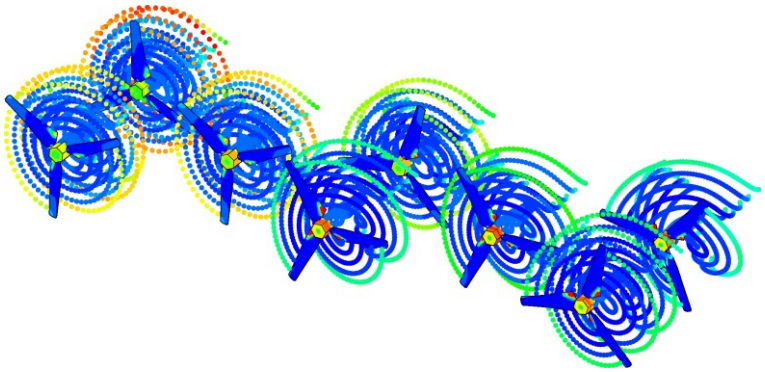

Figure 13. Farm modelling example with eight turbines by our numerical tool.

5. Acknowledgements

The authors would like to thank Haute-Normandie Regional Council for their financial support of co-financed PhD theses, as well as the CRIHAN (Centre des Ressources Informatiques de Haute-Normandie) for making their numerical resources available to us. The numerical software was originally designed for aeronautic purposes as part of project with Aircelle and Région Haute-Normandie. We would also like to thank Thomas Bacchetti and Jean-Valéry Facq for their precious help in the present work.

6. References

BALTAZAR J., FALCÃO DE CAMPOS J. A. C. (2008). *Hydrodynamic analysis of a horizontal axis marine current turbine with a boundary element method.* 27th OMAE Conference, Estoril (Portugal), pp 883–893.

BATTEN W., BAHAJ A., MOLLAND A., CHAPLIN J. (2008), *The prediction of the hydrodynamic performance of marine current turbines.* Renewable Energy, vol. 33, n° 5, pp 1085−1096.

MAGANGA F. (2011). *Caractérisation numérique et expérimentale des effets engendrés par l'implantation d'hydroliennes dans le milieu marin*. Thèse, IFREMER & Université du Havre, 236 p.

MAGANGA F., GERMAIN G., KING J., PINON G., RIVOALEN E. (2010). *Experimental characterisation of flow effects on marine current turbine behaviour and on its wake properties*. IET Renewable Power Generation, vol. 4, n° 6, pp 498–509.

MYERS L., BAHAJ A., RETZLER C., RICCI P., DHEDIN J.-F. (2010). *Inter-device spacing issues within wave and tidal energy converter arrays*. 3rd ICOE, Bilbao.

PINON G., BRATEC H., HUBERSON S., PIGNOT G., RIVOALEN E. (2005). *Vortex method for simulation of a 3D round jet in a cross-stream*. Journal of Turbulence, vol. 6, n° 18, pp 1–25.

PINON G., MYCEK P., GERMAIN G., RIVOALEN E. (2012). *Numerical Simulation of the Wake of Marine Current Turbines with a Particle Method*. Renewable Energy, vol. 46, pp 111–126.

RAWLINSON-SMITH R., BRYDEN I., FOLLEY M., MARTIN V., STALLARD T., STOCK-WILLIAMS C., WILLDEN R. (2010). *The Perawat project: Performance assessment of wave and tidal array systems*. 3rd International Conference on Ocean Energy (ICOE), Bilbao (Espagne).